Int. J. Solids Structures, 1972, Vol. 8, pp. 69 to 91. Pergamon Press. Printed in Great Britain

VIBRATION AND STABILITY OF CRACKED RECTANGULAR PLATES†

B. STAHL‡ and L. M. KEER§

Northwestern University, Evanston, Illinois

Abstract—The present paper deals with eigenvalue problems of cracked rectangular plates. Vibration and buckling problems are solved for a plate with a crack emanating from one edge and for a plate with a centrally located internal crack. The problems are formulated as dual series equations and reduced to homogeneous Fredholm integral equations of the second kind. The singularity of the solution in each case is isolated and treated analytically. Numerical results for the natural frequencies and moment distributions are compared with the work of other investigators. Vibration and buckling mode shapes are also illustrated for a cracked plate.

INTRODUCTION

THE objective of the present paper is to develop and demonstrate a method for determining the natural frequencies and buckling loads of rectangular plates with mixed boundary conditions arising from cracks. The plates are of uniform thickness and are simply supported along the four outer edges. Two cracked configurations are considered: a stationary crack penetrating the plate from one edge, and a centrally located internal crack.

Recently, Keer and Sve [1] have given a rigorous treatment of the symmetric bending of a cracked rectangular plate due to a static, uniform, transverse load. They formulated the problem as dual series equations and used a modification of the technique by Westmann and Yang [2] to obtain a solution in terms of a Fredholm integral equation of the second kind. Three cases were studied in their paper: two collinear external cracks of equal length, an internal crack centrally located and a single external crack. The dual series equation solution techniques presented by Keer and Sve are applied here to corresponding vibration and buckling problems. In addition, solutions to the more difficult problems associated with antisymmetric bending are given here.

A vibration analysis of a cracked rectangular plate has been made by Lynn and Kumbasar [3], who used a Green's function approach to obtain a Fredholm integral equation of the first kind. The subdomain method [4] was employed to satisfy the boundary conditions. No attempt was made to account for the singularity of the solution. A comparison of their numerical work with results obtained by the present method is made in this paper.

Numerical treatments of plates with mixed boundary conditions are given by Chen and Pickett [5, 6]. A survey of numerical methods for solving plate bending problems has been made by Leissa *et al.* [7]. It was concluded there that discontinuous boundary conditions are poorly approximated without the use of appropriate singularity functions. The work in this paper tends to confirm this conclusion.

† Presented at the Third Canadian Congress of Applied Mechanics, the University of Calgary (1971).
‡ Currently Senior Research Engineer, AMOCO Production Company, Tulsa, Oklahoma.
§ Professor of Civil Engineering.

A large amount of literature is available concerning mixed boundary value problems of infinite plates. Although the present analyses deal with finite plates, the solution of infinite plate problems provides the correct singularity to be used in the vicinity of the mixed condition. The local behavior at the point of discontinuity of the boundary conditions must be the same for both finite and infinite plates. For a plate containing a crack, the nature of the singularity may be deduced from the paper by Goodier [8] by considering the crack as a limiting case of an elliptical hole. The complex variable method as illustrated by Sih *et al.* [9] in conjunction with the paper by Yu [10] may also be used to deduce the nature of the singularity. In addition, the Fadle eigenfunction expansion technique employed by Williams [11, 12] may be used. From these methods, it is found that the moment stress resultant is singular as the inverse square root of the distance from the base of the crack. It will be shown that these singularities are indeed properly incorporated.

The present work is restricted to elementary plate theory, with the notation given by Timoshenko and Woinowsky-Krieger [13]. Since the plates are finite, the problems are formulated by means of Fourier series. The mixed boundary conditions lead to dual series equations with a weight function. The dual series equations are then converted by means of certain integral representations to a homogeneous Fredholm integral equation of the second kind from which the natural frequencies, the buckling parameter and the auxiliary function $\theta(\rho)$ are determined. The eigenfunctions (mode shapes) may be computed by use of $\theta(\rho)$.

PLATE WITH CRACK EMANATING FROM ONE EDGE

In this section problems involving the vibration and stability of plates with a crack emanating from one edge will be investigated. The various problems can also be considered as *internal* crack problems with an appropriate continuation of the plate. The partial differential equation which governs the free transverse motion $w_0(x, y, t)$ of a plate as shown in Fig. 1(a)† is given by

$$\nabla^4 w_0 + \frac{\mu}{D}\frac{\partial^2 w_0}{\partial t^2} = 0. \tag{1}$$

Letting

$$w_0(x, y, t) = w(x, y)\exp(i\Omega t), \tag{2}$$

the time dependence can be eliminated so as to obtain

$$\nabla^4 w - \frac{\mu}{D}\Omega^2 w = 0. \tag{3}$$

Utilizing the Levy-Nadai approach [13] for plates simply supported on two opposite edges, substitution of the partial expansion

$$w = \sum_{m=1,2,\ldots}^{\infty} Y_m(y)\sin(mx) \tag{4}$$

† The coordinates and dimensions shown on the plate geometry figures are scaled by the factor $\pi/\bar{a}$, where $\bar{a}$ is the actual plate length. Actual (barred) coordinates and dimensions are obtained by use of $\bar{x} = \bar{a}x/\pi$, $\bar{y} = \bar{a}y/\pi$, $\bar{b} = \bar{a}b/\pi$, $\bar{c} = \bar{a}c/\pi$ and $\bar{c}_1 = \bar{a}c_1/\pi$.

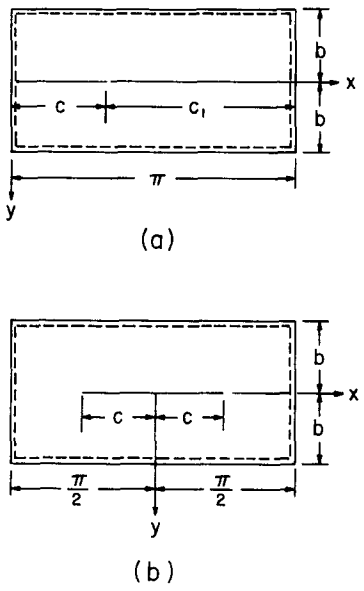

FIG. 1. Geometry of cracked plates.

into (3) leads to an ordinary differential equation for Y_m which has as its general solution

$$Y_m(y) = \frac{1}{D}[A_m \sinh(r_1 y) + B_m \cosh(r_1 y) + C_m \sinh(r_2 y) + D_m \cosh(r_2 y)] \tag{5}$$

where

$$\left.\begin{aligned} r_1 &= [k\Omega + m^2]^{\frac{1}{2}}, \\ r_2 &= [-k\Omega + m^2]^{\frac{1}{2}}, \\ k &= [\mu/D]^{\frac{1}{2}}. \end{aligned}\right\} \tag{6}$$

The buckling and vibration problems are very similar because the governing differential equations are almost identical and the same boundary conditions are applicable. By applying a uniform compressive load T on the edges perpendicular to the crack [see Fig. 1(a)], the governing partial differential equation may be written as

$$\nabla^4 w + \frac{T}{D}\frac{\partial^2 w}{\partial x^2} = 0. \tag{7}$$

By use of a partial expansion such as that given by equation (4), an ordinary differential equation can be developed for Y_m which has the solution

$$Y_m(y) = \frac{1}{D}[A_m \sinh(\rho_1 y) + B_m \cosh(\rho_1 y) + C_m \sinh(\rho_2 y) + D_m \cosh(\rho_2 y)] \tag{8}$$

where

$$\left.\begin{aligned} \gamma &= \pi/2b \\ \rho_1 &= [mp\gamma + m^2]^{\frac{1}{2}} \\ \rho_2 &= [-mp\gamma + m^2]^{\frac{1}{2}} \\ p\gamma &= \sqrt{(T/D)}. \end{aligned}\right\} \tag{9}$$

By comparing equations (8), (9) with (5), (6), it is evident that the buckling problem can be obtained from the vibration problem by redefining r_1 and r_2 according to (9) and by replacing $k\Omega$ with $mp\gamma$.

As is evident from Fig. 1(a) for all problems considered in this section, the following boundary conditions hold:

$$w, \frac{\partial^2 w}{\partial x^2} = 0, |y| \leq b, \qquad x = 0, \pi \tag{10}$$

$$w, \frac{\partial^2 w}{\partial y^2} = 0, |y| = b, \qquad 0 \leq x \leq \pi. \tag{11}$$

Boundary conditions (10), (11) express the fact that the edges $x = 0, \pi$ and $y = \pm b$ are simply supported. The remaining boundary conditions for each of the problems to be considered are obtained by focusing attention on the line $y = 0$.

(a) *Symmetric vibration of plate with crack from one edge*

The boundary conditions appropriate to this case of mode shapes symmetric about $y = 0$ are given by (10), (11) and the following:

$$V_y \sim \frac{\partial}{\partial y}\left[\frac{\partial^2 w}{\partial y^2} + (2-\nu)\frac{\partial^2 w}{\partial x^2}\right] = 0, \qquad y = 0, \qquad 0 \leq x \leq \pi \tag{12}$$

$$\frac{\partial w}{\partial y} = 0, \qquad y = 0, \qquad c < x \leq \pi \tag{13}$$

$$M_{yy} \sim \frac{\partial^2 w}{\partial y^2} + \nu\frac{\partial^2 w}{\partial x^2} = 0, \qquad y = 0, \qquad 0 \leq x < c. \tag{14}$$

Boundary conditions (12), (13) in $c < x \leq \pi$ follow from symmetry conditions and (12), (14) in $0 \leq x < c$ arise from the stress free condition on the face of the crack.

By use of the partial expansion given in (4), it is seen that (10) is automatically satisfied. Boundary conditions (11) and (12) lead to the relations

$$A_m = r_2[k\Omega + (1-\nu)m^2]C_m / r_1[k\Omega - (1-\nu)m^2] \tag{15}$$

$$B_m = -r_2[k\Omega + (1-\nu)m^2]\tanh(r_1 b)C_m / r_1[k\Omega - (1-\nu)m^2] \tag{16}$$

$$D_m = -\tanh(r_2 b)C_m. \tag{17}$$

The problem is therefore reduced to the determination of the constants C_m. The remaining boundary conditions (13), (14) are mixed with respect to the slope and moment, and they are written as the dual series equations

$$\sum_{m=1,2,\ldots}^{\infty} P_m \sin(mx) = 0, \qquad c < x \leq \pi \tag{18}$$

$$\sum_{m=1,2,\ldots}^{\infty} m[1+F_m(\Omega)]P_m \sin(mx) = 0, \qquad 0 \leq x < c \tag{19}$$

where P_m and $F_m(\Omega)$ are given by

$$P_m = 2r_2 k\Omega[k\Omega-(1-\nu)m^2]^{-1}C_m, \tag{20}$$

$$1+F_m(\Omega) = [(1-\nu)(\nu+3)mk\Omega]^{-1}\left\{\frac{\tanh(r_1 b)}{r_1}[k\Omega+(1-\nu)m^2]^2 - \frac{\tanh(r_2 b)}{r_2}[k\Omega-(1-\nu)m^2]^2\right\}. \tag{21}$$

As $m \to \infty$, the weight function $F_m(\Omega)$ approaches zero as m^{-4}. The constant 1 in the bracketed term of (19) serves to isolate the singularity associated with the static problem of a cracked plate strip infinite in the y-coordinate. This is readily seen to be the case since $F_m(\Omega) \to 0$ by letting $b \to \infty$ and then letting $\Omega \to 0$.

The dual series equations (18), (19) may be reduced to a single integral equation by representing the unknown coefficients P_m by a finite Hankel transform

$$P_m = \int_0^c t\varphi(t)J_1(mt)\,\mathrm{d}t, \tag{22}$$

where $J_1(mt)$ is the Bessel function of the first kind and first order. By substituting P_m into the first of the dual series equations, interchanging the order of summation and integration, and using the identity

$$\sum_{m=1,2,\ldots}^{\infty} J_1(mt)\sin(mx) = xt^{-1}(t^2-x^2)^{-\frac{1}{2}}H(t-x), \tag{23}$$

where $H(t-x)$ is the Heaviside function, it is easily seen that (18) is automatically satisfied. Equation (23) and all of the integral representations of series involving Bessel functions used throughout this paper may be derived by appropriate contour integrations around the first quadrant of the complex plane [1].

Integrating (19) once with respect to x and substituting (22) yields, after an interchange in the order of summation and integration,

$$\int_0^c t\varphi(t) \sum_{m=1,2,\ldots}^{\infty} [1+F_m(\Omega)]J_1(mt)\cos(mx)\,\mathrm{d}t = 0, \qquad 0 \leq x < c. \tag{24}$$

By utilizing the integral representation

$$\sum_{m=1,2,\ldots}^{\infty} J_1(mt)\cos(mx) = t^{-1} - xt^{-1}(x^2-t^2)^{-\frac{1}{2}}H(x-t) - 2\int_0^{\infty} [\exp(2\pi s)-1]^{-1} I_1(ts)\cosh(xs)\,\mathrm{d}s, \tag{25}$$

equation (24) is put into the form of Abel's integral equation

$$\int_0^x \varphi(t)(x^2-t^2)^{-\frac{1}{2}}\,\mathrm{d}t = h(x), \tag{26}$$

where

$$\varphi(t) = \frac{2}{\pi}\frac{\mathrm{d}}{\mathrm{d}t}\int_0^t xh(x)(t^2-x^2)^{-\frac{1}{2}}\,\mathrm{d}x. \tag{27}$$

$I_1(ts)$ in (25) is the modified Bessel function of the first kind and first order. With the help of certain identities found in [14], the final result becomes

$$\theta(\rho)+\int_0^1 K(\rho, r)\theta(r)\,\mathrm{d}r = 0, \qquad 0 \le \rho \le 1, \tag{28}$$

where $\theta(\rho) = \varphi(c\rho)$. The kernel of the integral equation is written as

$$K(\rho, r) = c^2 r\left\{\sum_{m=1,2,\ldots}^{\infty} F_m(\Omega)mJ_1(mcr)J_1(m\rho c) + 2\int_0^\infty s[\exp(2\pi s)-1]^{-1}I_1(rsc)I_1(\rho sc)\,\mathrm{d}s\right\}. \tag{29}$$

It should be remarked that (24) should include an arbitrary constant of integration as a result of integrating (19) with respect to x. In the process of solving Abel's integral equation, however, the arbitrary constant has no effect and may be ignored.

The singularity of M_{yy} at the crack tip may be verified by considering the second dual series equation (19), which represents M_{yy} on $y = 0$, and by substituting equation (22) written in the form

$$P_m = -m^{-1}c\varphi(c)J_0(mc)+m^{-1}\int_0^c J_0(mt)\frac{\mathrm{d}}{\mathrm{d}t}[t\varphi(t)]\,\mathrm{d}t. \tag{30}$$

It may be shown that in the vicinity of the crack tip,

$$M_{yy}|_{y=0} \sim \frac{-c\varphi(c)}{\sqrt{2c\sqrt{\varepsilon}}}+0(\varepsilon^{\frac{1}{4}}), \tag{31}$$

and thus the moment is square root singular near the crack tip which is in complete agreement with the references cited in the Introduction.

For the purpose of calculating the moment distribution along the uncracked segment, it is convenient to write equation (19) in the form

$$M_{yy}|_{y=0} \sim -\frac{\mathrm{d}}{\mathrm{d}x}\sum_{m=1,2,\ldots}^{\infty} P_m\cos(mx)+\sum_{m=1,2,\ldots}^{\infty} mF_m(\Omega)P_m\sin(mx). \tag{32}$$

By substituting (22) into (32) and using the integral representation of (25), equation (32) may be written as

$$M_{yy}(x,0) \sim c^2\int_0^1 K(x,\rho)\theta(\rho)\,\mathrm{d}\rho+\sum_{m=1,2,\ldots}^{\infty} mF_m(\Omega)P_m\sin(mx),\ x > c, \tag{33}$$

where

$$K(x,\rho) = -c\rho^2[x^2-c^2\rho^2]^{-\frac{3}{2}} + 2\rho\int_0^\infty [\exp(2\pi s)-1]^{-1} I_1(c\rho s)s\sinh(xs)\,\mathrm{d}s \tag{34}$$

and

$$P_m = c^2\int_0^1 \rho\theta(\rho)J_1(mc\rho)\,\mathrm{d}\rho. \tag{35}$$

The moment field at points other than $y = 0$ can also be calculated but with a little more difficulty. An expression for M_{yy} on $y > 0$ can be written in the form

$$M_{yy} \sim \sum_{m=1,2,\ldots}^{\infty} m[\exp(-my)+F_m(\Omega, y)]P_m \sin(mx). \tag{36}$$

For large y, the above series can be summed as it stands. For $y \ll b$, the series converges too slowly because of the moment singularity. Therefore it is necessary to isolate the series corresponding to the first term in the brackets and to substitute appropriate integral representations. A procedure for integral equations analogous to the one required here for series equations was used by Sve and Keer [15] in calculating punch isochromatics.

(b) *Antisymmetric vibration of plate with crack from one edge*

The shape function is given by (4) and the coordinate system is shown in Fig. 1(a). Boundary conditions (10), (11) again hold and the boundary conditions on the line $y = 0$ are given by

$$M_{yy} \sim \frac{\partial^2 w}{\partial y^2}+\nu\frac{\partial^2 w}{\partial x^2} = 0, \qquad y = 0, \qquad 0 \le x \le \pi \tag{37}$$

$$w = \frac{\partial w}{\partial x} = \frac{\partial^2 w}{\partial x^2} = 0, \qquad y = 0, \qquad c < x \le \pi \tag{38}$$

$$V_y \sim \frac{\partial}{\partial y}\left[\frac{\partial^2 w}{\partial y^2}+(2-\nu)\frac{\partial^2 w}{\partial x^2}\right] = 0, \qquad y = 0, \qquad 0 \le x < c. \tag{39}$$

It should be noted that the above boundary conditions are also applicable for a plate which is partly free and partly simply supported along the line $y = 0$.

By applying (11) and (37), one is led to the relations

$$A_m = -\coth(r_1 b)B_m \tag{40}$$

$$C_m = \coth(r_2 b)B_m[k\Omega+(1-\nu)m^2]/[-k\Omega+(1-\nu)m^2] \tag{41}$$

$$D_m = -[k\Omega+(1-\nu)m^2]B_m/[-k\Omega+(1-\nu)m^2]. \tag{42}$$

The mixed boundary conditions (38) and (39) lead to dual series equations given by (18) and (19), but where P_m and $F_m(\Omega)$ are given by

$$P_m = 2k\Omega m^2 B_m/[-k\Omega+(1-\nu)m^2] \tag{43}$$

and

$$1+F_m(\Omega) = [m^3 k\Omega(\nu+3)(\nu-1)]^{-1}\{r_1 \coth(r_1 b)[k\Omega-(1-\nu)m^2]^2 - r_2 \coth(r_2 b)[k\Omega+(1-\nu)m^2]^2\}. \tag{44}$$

The first of the dual series equations for this case represents the condition $\partial^2 w/\partial x^2 = 0$ on $y = 0$ and $c < x \leq \pi$, which facilitates the introduction of the appropriate singularity at the tip of the crack, but is not sufficient to insure that $w = \partial w/\partial x = 0$ on $y = 0, c < x \leq \pi$. Hence, the auxiliary condition that $\partial w/\partial x = 0$ on $y = 0$ and $x = \pi$ is imposed.

The appropriate representation for P_m which results in the proper singularity and at the same time permits the auxiliary condition to be satisfied, is

$$P_m = EJ_1(mc) + \int_0^c t\varphi(t)J_1(mt)\,dt, \qquad m = 1, 2, \ldots \tag{45}$$

The constant E is determined by imposing

$$\frac{\partial w}{\partial x}(\pi, 0) = \sum_{m=1,2,\ldots}^{\infty} m^{-1} P_m \cos m\pi = 0, \tag{46}$$

which leads to

$$E = \int_0^c t\varphi(t)k(t)\,dt, \tag{47}$$

where

$$k(t) = -\sum_{m=1,2,\ldots}^{\infty} m^{-1} J_1(mt)(-1)^m \Big/ \sum_{m=1,2,\ldots}^{\infty} m^{-1} J_1(mc)(-1)^m. \tag{48}$$

It can be shown that

$$\sum_{m=1,2,\ldots}^{\infty} m^{-1} J_1(mt)(-1)^m = -\frac{1}{4}t, \qquad 0 \leq t < \pi. \tag{49}$$

Hence,

$$k(t) = -t/c, \tag{50}$$

and substituting E into equation (45) results in

$$P_m = \int_0^c t\varphi(t)\left[J_1(mt) - \frac{t}{c}J_1(mc)\right] dt, \qquad m = 1, 2, \ldots \tag{51}$$

It is easily verified that the first of the dual series equations is automatically satisfied. By the procedure indicated in the previous case, the second of the dual series equations leads to (28) where

$$K(\rho, r) = c^2 r\left\{\sum_{m=1,2,\ldots}^{\infty} F_m(\Omega)[J_1(mcr) - rJ_1(mc)]mJ_1(mc\rho) + 2\int_0^{\infty} [\exp(2\pi s) - 1]^{-1}[I_1(scr) - rI_1(sc)]sI_1(sc\rho)\,ds\right\}. \tag{52}$$

The singularity of M_{xx} at the root of the crack may be verified in a manner analogous to the symmetric case. It is easily shown that

$$M_{xx}|_{y=0} \sim \sum_{m=1,2,\ldots}^{\infty} P_m \sin(mx). \tag{53}$$

Substituting (45) into (53) results in

$$M_{xx}|_{y=0} \sim E \sum_{m=1,2,\ldots}^{\infty} J_1(mc)\sin(mx) + \int_0^c t\varphi(t) \sum_{m=1,2,\ldots}^{\infty} J_1(mt)\sin(mx)\,dt. \tag{54}$$

The first term in (54) results in

$$M_{xx} \sim E(2c)^{-\frac{1}{2}}\varepsilon^{-\frac{1}{2}} + 0(\varepsilon^{\frac{1}{2}}) \tag{55}$$

in the vicinity of the root of the crack along $y = 0$.

(c) *Symmetric buckling of plate with crack from one edge and uniform load on edges perpendicular to crack*

It is evident that the buckling problem can be obtained from the vibration problem by redefinition of r_1 and r_2 according to equations (9) and by replacing $k\Omega$ with $mp\gamma$. Thus the values of A_m, B_m and D_m as given by (15)–(17) hold subject to this redefinition. The governing dual series equations may be immediately written as [see equations (18)–(21)]

$$\sum_{m=1,2,\ldots}^{\infty} P_m \sin(mx) = 0, \qquad c < x \leq \pi \tag{56}$$

$$\sum_{m=1,2,\ldots}^{\infty} m[1+F_m(p)]P_m \sin(mx) = 0, \qquad 0 \leq x < c, \tag{57}$$

where

$$P_m = 2\rho_2 mp\gamma[mp\gamma - (1-\nu)m^2]^{-1}C_m, \tag{58}$$

$$1+F_m(p) = [(1-\nu)(\nu+3)m^2p\gamma]^{-1}\left\{\frac{\tanh(\rho_1 b)}{\rho_1}[mp\gamma+(1-\nu)m^2]^2 - \frac{\tanh(\rho_2 b)}{\rho_2}[mp\gamma-(1-\nu)m^2]^2\right\}. \tag{59}$$

Solving the above dual series equations in the same manner as the vibration case results in (28) where the kernel is given by

$$K(\rho, r) = c^2 r\left\{\sum_{m=1,2,\ldots}^{\infty} F_m(p)mJ_1(mcr)J_1(mc\rho) + 2\int_0^{\infty} s[\exp(2\pi s)-1]^{-1}I_1(rsc)I_1(\rho sc)\,ds\right\}. \tag{60}$$

The difficulty with this result is that as $m \to \infty$, $F_m(p) \to 0$ as m^{-2} and hence the series in (60) converges slowly. Since the series must be evaluated for each trial value of the parameter p, it seems desirable to improve the convergence. By a procedure similar to that used by

Sih and Loeber [16] in a problem involving a penny-shaped crack, the second of the dual series equations may be written as

$$\sum_{m=1,2,\ldots}^{\infty} m\left[1-\frac{\gamma^2 p^2 h(v)}{m^2+1}+G_m(p)\right]P_m \sin(mx)=0, \qquad 0 \le x < c, \tag{61}$$

where

$$h(v)=\frac{5v^2+2v+1}{8(1-v)(3+v)} \tag{62}$$

and

$$G_m(p)=\frac{\gamma^2 p^2 h(v)}{m^2+1}+F_m(p). \tag{63}$$

It can be shown that as $m \to \infty$, $G_m(p) \to 0$ as m^{-4}. It seems reasonable to write the kernel in the form

$$\begin{aligned} K(\rho, r) = c^2 r\Bigg\{ & \sum_{m=1,2,\ldots}^{\infty} G_m(p) J_1(mcr) m J_1(mc\rho) - \gamma^2 p^2 h(v) \sum_{m=1,2,\ldots}^{\infty} [m^2+1]^{-1} \\ & \times J_1(mcr) m J_1(mc\rho) + 2\int_0^{\infty} [\exp(2\pi s)-1]^{-1} I_1(crs) s I_1(\rho sc)\, \mathrm{d}s \Bigg\}. \end{aligned} \tag{64}$$

The second series in (64) coverges slowly. However, it need be calculated only once for each crack length and therefore (64) provides a relatively efficient means of computing the critical load parameter.

By means of a contour integration of

$$\frac{\exp(i\pi w) J_1(tw)\cos(xw)}{(w^2+1)\sin(\pi w)}$$

around the first quadrant, the following identity can be derived:

$$\begin{aligned} \sum_{m=1,2,\ldots}^{\infty} [m^2+1]^{-1} J_1(mt)\cos(mx) = & \int_0^{\infty} \frac{J_1(tu)\cos(xu)\,\mathrm{d}u}{u^2+1} \\ & + 2\int_0^{\infty} \frac{[\exp(2\pi v)-1]^{-1} I_1(tv)\cosh(xv)\,\mathrm{d}v}{v^2-1}. \end{aligned} \tag{65}$$

By use of (65) and with the help of an identity found in [14, p. 694], the kernel of the integral equation may be written in the alternative form

$$\begin{aligned} K(\rho, r) = c^2 r\Bigg\{ & \sum_{m=1,2,\ldots}^{\infty} G_m(p) J_1(mcr) m J_1(mc\rho) \\ & + 2\int_0^{\infty} [\exp(2\pi s)-1]^{-1} I_1(crs) s I_1(\rho cs)\,\mathrm{d}s \\ & - \gamma^2 p^2 h(v) \begin{bmatrix} I_1(cr)K_1(c\rho), & \rho \ge r \\ K_1(cr)I_1(c\rho), & r \ge \rho \end{bmatrix} \\ & + 2\gamma^2 p^2 h(v)\int_0^{\infty} [\exp(2\pi s)-1]^{-1}[s^2-1]^{-1} I_1(crs) s I_1(c\rho s)\,\mathrm{d}s \Bigg\}. \end{aligned}$$

The above kernel requires the evaluation of a principal value integral. Since there is no apparent advantage in its use, equation (64) was used for the numerical calculations.

PLATE WITH INTERNAL CRACK

In this section problems involving the vibration and stability of plates with an internal crack will be considered, the geometry of which is given in Fig. 1(b). Only the cases of vibration and buckling *symmetric* with respect to the y-axis will be considered since the cases that are antisymmetric about the y-axis have essentially been solved in the preceding section if the plate dimension is reduced by half.

If the plate is simply supported on all four sides, the corresponding boundary conditions are expressed by

$$w, \frac{\partial^2 w}{\partial x^2} = 0, \qquad |y| \leq b, \qquad x = -\frac{\pi}{2}, \frac{\pi}{2} \tag{66}$$

$$w, \frac{\partial^2 w}{\partial y^2} = 0, \qquad |y| = b, \qquad -\frac{\pi}{2} \leq x \leq \frac{\pi}{2}. \tag{67}$$

In view of the above boundary conditions, the shape function is taken as the partial expansion

$$w = \sum_{m=1,3,\ldots}^{\infty} Y_m(y) \cos(mx), \tag{68}$$

where $Y_m(y)$ is given by (5).

(a) *Symmetric–symmetric vibration of plate with internal crack*

The first case to be considered is that in which the mode shapes are symmetric about both coordinate axes. Considering the lower right-hand quadrant of the plate, the additional boundary conditions resulting from the presence of the crack may be expressed by

$$V_y \sim \frac{\partial}{\partial y}\left[\frac{\partial^2 w}{\partial y^2} + (2-\nu)\frac{\partial^2 w}{\partial x^2}\right] = 0, \qquad y = 0, \qquad 0 \leq x \leq \frac{\pi}{2} \tag{69}$$

$$\frac{\partial w}{\partial y} = 0, \qquad y = 0, \qquad c < x < \frac{\pi}{2} \tag{70}$$

$$M_{yy} \sim \frac{\partial^2 w}{\partial y^2} + \nu \frac{\partial^2 w}{\partial x^2} = 0, \qquad y = 0, \qquad 0 \leq x < c. \tag{71}$$

By using equations (67) and (69) three relations may be found between the unknowns A_m, B_m, C_m and D_m and they are those given by (15)–(17). The mixed boundary conditions (70), (71) lead to the dual series equations

$$\sum_{m=1,3,\ldots}^{\infty} P_m \cos(mx) = 0, \qquad c < x \leq \frac{\pi}{2} \tag{72}$$

$$\sum_{m=1,3,\ldots}^{\infty} m[1 + F_m(\Omega)] P_m \cos(mx) = 0, \qquad 0 \leq x < c \tag{73}$$

where P_m and $F_m(\Omega)$ are given by equations (20) and (21), respectively.

The representation for P_m, which introduces a square root moment singularity at the crack tip, is given by

$$P_m = \int_0^c \varphi(t) J_0(mt)\, dt, \tag{74}$$

where $J_0(mt)$ is the Bessel function of the first kind and zeroth order. It can be easily verified that (74) satisfies the first of the dual series equations. Integrating the second of the equations once with respect to x between the limits of 0 and x, and substituting (74) yields, after an interchange in the order of summation and integration,

$$\int_0^c \varphi(t) \sum_{m=1,3,\ldots}^{\infty} [1 + F_m(\Omega)] J_0(mt) \sin(mx)\, dt = 0, \qquad 0 \le x < c. \tag{75}$$

By use of an integral representation for the first term in (75), it can be put into the form of Abel's integral equation. With the help of identities found in [14], the final result becomes (28), where

$$K(\rho, r) = 2c^2\rho \left\{ \sum_{m=1,3,\ldots}^{\infty} F_m(\Omega) J_0(mcr) m J_0(mc\rho) + \int_0^{\infty} [\exp(\pi s) + 1]^{-1} s I_0(rsc) I_0(\rho sc)\, ds \right\}. \tag{76}$$

(b) *Symmetric–antisymmetric vibration of plate with internal crack*

For this case, the boundary conditions which are applicable, in addition to those given by (66) and (67), are

$$M_{yy} \sim \frac{\partial^2 w}{\partial y^2} + \nu \frac{\partial^2 w}{\partial x^2} = 0, \qquad y = 0, \qquad 0 \le x \le \frac{\pi}{2} \tag{77}$$

$$w = \frac{\partial w}{\partial x} = \frac{\partial^2 w}{\partial x^2} = 0, \qquad y = 0, \qquad c < x \le \frac{\pi}{2} \tag{78}$$

$$V_y \sim \frac{\partial}{\partial y}\left[\frac{\partial^2 w}{\partial y^2} + (2 - \nu)\frac{\partial^2 w}{\partial x^2}\right] = 0, \qquad y = 0, \qquad 0 \le x < c. \tag{79}$$

The above boundary conditions are derived from considerations of the antisymmetry of the deflection function in the y-coordinate and the stress free state along the face of the crack.

The shape function is given by (68) and satisfies boundary conditions (66). Upon application of the boundary conditions (67) and (77), the three relations between the unknowns A_m, B_m, C_m and D_m are found to be given by equations (40)–(42). The mixed boundary conditions above lead to the dual series equations

$$\sum_{m=1,3,\ldots}^{\infty} P_m \sin(mx) = 0, \qquad c < x \le \frac{\pi}{2} \tag{80}$$

$$\sum_{m=1,3,\ldots}^{\infty} m^2 [1 + F_m(\Omega)] P_m \cos(mx) = 0, \qquad 0 \le x < c \tag{81}$$

where

$$P_m = 2k\Omega mB_m/[-k\Omega+(1-\nu)m^2] \tag{82}$$

and where $F_m(\Omega)$ is defined by (44). The first of the dual series equations above arises from $\partial w/\partial x = 0$ on $y = 0, c < x < \pi/2$. This condition is used rather than the other two in (78) because it permits the appropriate singularity at the crack tip to be introduced. However, all conditions of (78) are automatically satisfied since the shape function equals zero at $x = \pi/2$.

The solution to the above dual series equations proceeds by taking the finite Hankel transform of (22) as the appropriate representation for P_m. The first of the dual series equations will be automatically satisfied. The second of the dual series equations is integrated twice with respect to x. The first integration takes place between the limits of zero and x. A constant of integration which appears with the second integration may be ignored for reasons given earlier. With an appropriate contour integration and by use of certain identities found in [14] the second of the dual series equations finally leads to a homogeneous Fredholm integral equation of the second kind as given by (28). The kernel of this integral equation is written as

$$K(\rho, r) = 2c^2 r\left\{\sum_{m=1,3,\ldots}^{\infty} F_m(\Omega)J_1(mcr)mJ_1(mc\rho) - \int_0^{\infty} [\exp(\pi s)+1]^{-1} I_1(rsc)sI_1(\rho sc)\,\mathrm{d}s\right\}. \tag{83}$$

(c) *Symmetric–symmetric buckling of plate with internal crack and uniform load on edges perpendicular to crack*

The analogy between buckling and vibration has been pointed out earlier. The dual series equations may be written down immediately as

$$\sum_{m=1,3,\ldots}^{\infty} P_m \cos(mx) = 0, \qquad c < x \leq \frac{\pi}{2} \tag{84}$$

$$\sum_{m=1,3,\ldots}^{\infty} m\left[1-\frac{\gamma^2 p^2 h(\nu)}{m^2+1}+G_m(p)\right]P_m \cos(mx) = 0, \qquad 0 \leq x < c \tag{85}$$

where $h(\nu)$ and $G_m(p)$ are defined by (62) and (63). The solution to the dual series equations may also be written by inspection. A homogeneous Fredholm integral equation of the second kind is obtained as in (28) and the kernel is written as

$$K(\rho, r) = 2c^2\rho\left\{\sum_{m=1,3,\ldots}^{\infty} G_m(p)J_0(mcr)mJ_0(mc\rho) - \gamma^2 p^2 h(\nu)\sum_{m=1,3,\ldots}^{\infty}(m^2+1)^{-1}J_0(mcr)mJ_0(mc\rho) + \int_0^{\infty}[\exp(\pi s)+1]^{-1}sI_0(rsc)I_0(\rho sc)\,\mathrm{d}s\right\}. \tag{86}$$

NUMERICAL PROCEDURE AND RESULTS

Both the vibration and buckling problems have been reduced to the solution of a homogeneous Fredholm integral equation of the second kind. The kernel of the integral equation contains the unknown parameter being sought, e.g. the frequency of free vibration. Because of the complexity of the kernel, the integral equation is treated numerically by reducing it to a system of homogeneous algebraic equations using Simpson's rule. In matrix notation, the integral equation may be written as

$$[I]\{\theta\}+[\bar{K}(\Omega)]\{\theta\} = 0 \tag{87}$$

where $[I]$ is the unit matrix and $\bar{K}(\Omega)$ is the discretized kernel of the integral equation. Defining

$$[A(\Omega)] = [I]+[\bar{K}(\Omega)], \tag{88}$$

a nontrivial solution of (88) is found by searching for that value of Ω which causes the determinant of the matrix A to vanish. The frequency factor f is related to the frequency Ω by

$$k\Omega = f(\pi/\bar{a})^2(1+\gamma^2). \tag{89}$$

In all calculations the value of Poisson's ratio was 0·3 ($\nu = 0{\cdot}3$).

The search procedure for finding the frequency is a trial and error process. First, a crack length is specified and the matrix A of (88) is calculated for several values of frequency. An estimate of the trial frequencies can be obtained by calculating the upper and lower bounds, i.e. the uncracked and completely cracked cases, by use of standard techniques. The determinant of the matrix A corresponding to each value of the frequency is then computed. If the estimates of the trial frequencies are reasonably good, a change in sign of the determinants would be observed and an approximate value of the frequency can be obtained by locating the crossing. Further trials can be used to pinpoint the value of the frequency.

A very efficient technique for obtaining the frequency is Muller's iterative method [17], which is a quadratic interpolation scheme for finding the roots. It has been used for all of the analyses presented here. Usually five or six evaluations of the matrix A were found to be sufficient for an accurate determination of the frequency or buckling factors.

In the calculation of the matrix A of (88), the infinite series of the kernel were evaluated to a relative error criterion of 1/5000, i.e. the series evaluation was terminated when the ratio of the absolute value of the last term calculated to the absolute value of the sum of all previous terms became less than 1/5000. Increasing the accuracy of the series evaluations did not improve the final results. The integrand of the infinite integral in the kernel is a monotonically increasing function up to some maximum. After the maximum is reached, the integrand decays exponentially. Simpson's rule was used in the evaluation of the infinite integrals and a sufficient number of intervals were used to ensure accurate results.

Another factor which affects the accuracy of the solution is the order of the matrix A. The numerical results for the crack cases are tabulated in Tables 1–8 and were obtained from eleventh-order matrices. For some crack lengths the fourth significant figure of the frequency factor for the higher modes may not be accurate.

TABLE 1. FREQUENCY FACTORS AND EIGENVALUE RATIOS FOR PLATE WITH CRACK FROM ONE EDGE. VIBRATION MODES SYMMETRIC IN y. $\gamma = 2{\cdot}0$

	Mode 1		Mode 2		Mode 3	
c/π	f	λ/λ_s	f	λ/λ_s	f	λ/λ_s
0·0	1·000(1)†	1·000	1·600(2)	1·000	2·600(3)	1·000
0·1	1·000	1·000	1·598	0·999	2·596	0·999
0·2	0·992	0·996	1·578	0·993	2·565	0·993
0·3	0·964	0·982	1·528	0·977	2·527	0·986
0·4	0·902	0·950	1·485	0·964	2·522	0·985
0·5	0·818	0·904	1·475	0·960	2·501	0·981
0·6	0·733	0·856	1·471	0·959	2·459	0·972
0·7	0·661	0·813	1·439	0·948	2·449	0·971
0·8	0·606	0·778	1·382	0·929	2·436	0·968
0·9	0·570	0·755	1·329	0·911	2·395	0·960
1·0	0·558(1)	0·747	1·308(2)	0·904	2·368(3)	0·954

† Numbers in parentheses indicate the number of semiwaves in the x coordinate.

TABLE 2. FREQUENCY FACTORS AND EIGENVALUE RATIOS FOR PLATE WITH CRACK FROM ONE EDGE. VIBRATION MODES ANTISYMMETRIC IN y. $\gamma = 2{\cdot}0$

	Mode 1		Mode 2		Mode 3	
c/π	f	λ/λ_s	f	λ/λ_s	f	λ/λ_s
0·0	3·400(1)†	1·000	4·000(2)	1·000	5·000(3)	1·000
0·1	3·400	1·000	3·991	0·999	4·997	1·000
0·2	3·386	0·998	3·932	0·991	4·820	0·982
0·3	2·917	0·926	3·545	0·941	4·416	0·940
0·4	2·028	0·772	3·521	0·938	4·385	0·937
0·5	1·492	0·662	3·416	0·924	4·015	0·896
0·6	1·165	0·585	2·870	0·847	3·852	0·878
0·7	0·951	0·529	2·319	0·761	3·790	0·871
0·8	0·801	0·485	1·915	0·692	3·371	0·821
0·9	0·692	0·451	1·620	0·636	2·877	0·759
1·0	0·558(1)	0·405	1·308(2)	0·572	2·368(3)	0·688

† Numbers in parentheses indicate the number of semiwaves in the x coordinate.

TABLE 3. BUCKLING FACTOR VS. CRACK LENGTH FOR PLATE WITH CRACK FROM ONE EDGE. $\gamma = 2{\cdot}0$

c/π	p
0·00	2·000(2)†
0·10	1·998
0·20	1·964
0·30	1·861
0·40	1·744
0·50	1·652
0·60	1·583
0·70	1·528
0·80	1·473
0·90	1·428
1·00	1·394(1)

† Numbers in parentheses indicate number of semiwaves in x coordinate.

TABLE 4. FREQUENCY FACTOR VS. CRACK LENGTH FOR PLATE WITH INTERNAL CRACK. VIBRATION MODES SYMMETRIC IN x AND SYMMETRIC IN y. $\gamma = 1{\cdot}0$

	Mode 1(a)	Mode 1(b)	Mode 3(a)
c/π	f	f	f
0·00	1·000(1)†	5·000(1)	5·000(3)
0·05	0·994	4·934	5·000
0·10	0·978	4·760	5·000
0·15	0·954	4·540	4·999
0·20	0·926	4·332	4·999
0·25	0·897	4·162	4·985
0·30	0·871	4·032	4·964
0·35	0·848	3·936	4·935
0·40	0·831	3·869	4·902
0·45	0·821	3·828	4·876
0·50	0·817(1)	3·814(1)	4·865(3)

† Numbers in parentheses indicate number of semiwaves in x coordinate.

TABLE 5. FREQUENCY FACTOR VS. CRACK LENGTH FOR PLATE WITH INTERNAL CRACK. VIBRATION MODES ANTISYMMETRIC IN x AND SYMMETRIC IN y. $\gamma = 1{\cdot}0$

	Mode 2(a)	Mode 2(b)	Mode 4
c/π	f	f	f
0·00	2·500(2)†	6·500(2)	8·500(4)
0·05	2·500	6·499	8·499
0·10	2·499	6·490	8·492
0·15	2·494	6·452	8·470
0·20	2·484	6·366	8·444
0·25	2·467	6·228	8·429
0·30	2·443	6·060	8·427
0·35	2·417	5·896	8·420
0·40	2·394	5·762	8·395
0·45	2·377	5·675	8·363
0·50	2·368(2)	5·625(2)	8·348(4)

† Numbers in parentheses indicate number of semiwaves in x coordinate.

TABLE 6. FREQUENCY FACTOR VS. CRACK LENGTH FOR PLATE WITH INTERNAL CRACK. VIBRATION MODES SYMMETRIC IN x AND ANTISYMMETRIC IN y. $\gamma = 1{\cdot}0$

	Mode 1(c)	Mode 3(b)	Mode 1(d)
c/π	f	f	f
0·00	2·500(1)†	6·500(3)	8·500(1)
0·05	2·499	6·498	8·494
0·10	2·491	6·463	8·392
0·15	2·456	6·288	7·890
0·20	2·362	5·656	7·143
0·25	2·180	4·827	6·842
0·30	1·924	4·326	6·672
0·35	1·652	4·085	6·467
0·40	1·407	3·971	6·149
0·45	1·192	3·909	5·700
0·49	1·007	—	5·235
0·50	0·817(1)	3·814(1)	4·865(3)

† Numbers in parentheses indicate number of semiwaves in x coordinate.

TABLE 7. FREQUENCY FACTOR VS. CRACK LENGTH FOR PLATE WITH INTERNAL CRACK. VIBRATION MODES ANTISYMMETRIC IN x AND ANTISYMMETRIC IN y. $\gamma = 1{\cdot}0$

c/π	Mode 2(c) f
0·00	4·000(2)†
0·05	4·000
0·10	4·000
0·15	3·997
0·20	3·982
0·25	3·938
0·30	3·829
0·35	3·626
0·40	3·330
0·45	2·983
0·50	2·368(2)

† Numbers in parentheses indicate number of semiwaves in x coordinate.

TABLE 8. BUCKLING FACTOR VS. CRACK LENGTH FOR PLATE WITH INTERNAL CRACK. $\gamma = 1{\cdot}0$

c/π	p
0·00	2·000(1)†
0·05	1·989
0·10	1·956
0·15	1·907
0·20	1·850
0·25	1·792
0·30	1·739
0·35	1·695
0·40	1·662
0·45	1·642
0·50	1·635(1)

† Numbers in parentheses indicate number of semiwaves in x coordinate.

The frequency factors for the plate with a crack from one edge are tabulated in Tables 1 and 2 as a function of crack length. The modes are numbered according to the number of semiwaves in the x-coordinate. In addition to the frequency factors, eigenvalue ratios are tabulated in order to facilitate a comparison with the figures given in Ref. [3]. The eigenvalue λ is related to the frequency factor f by

$$\Omega = f\left(\frac{\pi}{\bar{a}}\right)^2 [1+\gamma^2]\left[\frac{D}{\mu}\right]^{\frac{1}{2}} = \left[\frac{D}{\mu}\frac{\lambda^4}{\bar{a}^4}\right]^{\frac{1}{2}}. \tag{90}$$

The value λ_s for each mode equals λ evaluated at $c/\pi = 0$.

The solid lines on Figs. 2 and 3 represent the above tabular data in graphical form. The dashed lines are taken from Ref. [3]. The maximum difference between the solid and dashed line in mode 1 of the antisymmetric modes is about 11 per cent. Considering that the method

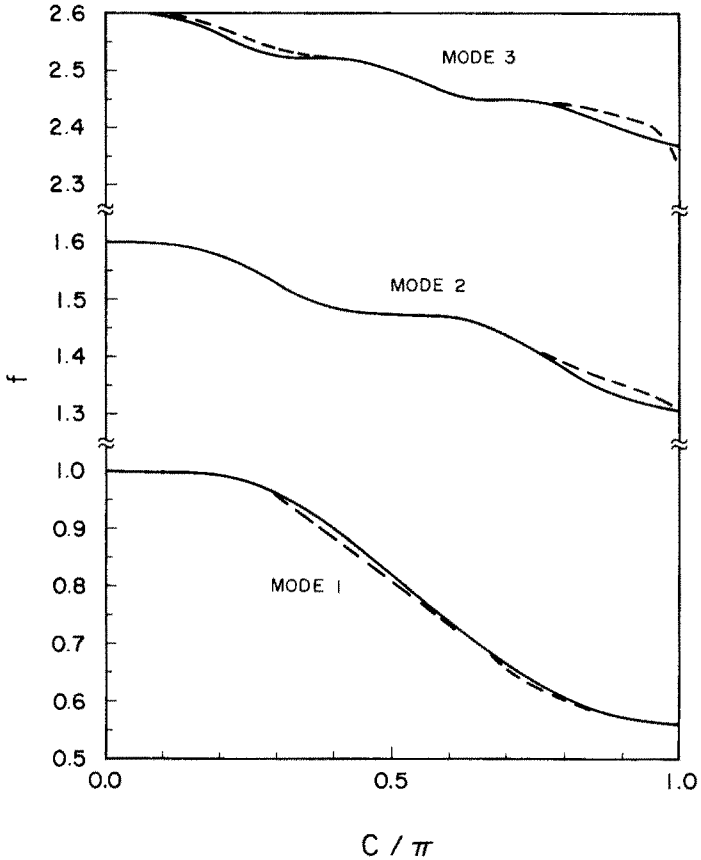

FIG. 2. Frequency factors vs. crack length for plate with crack from one edge. Vibration modes symmetric in y. $\gamma = 2{\cdot}0$.

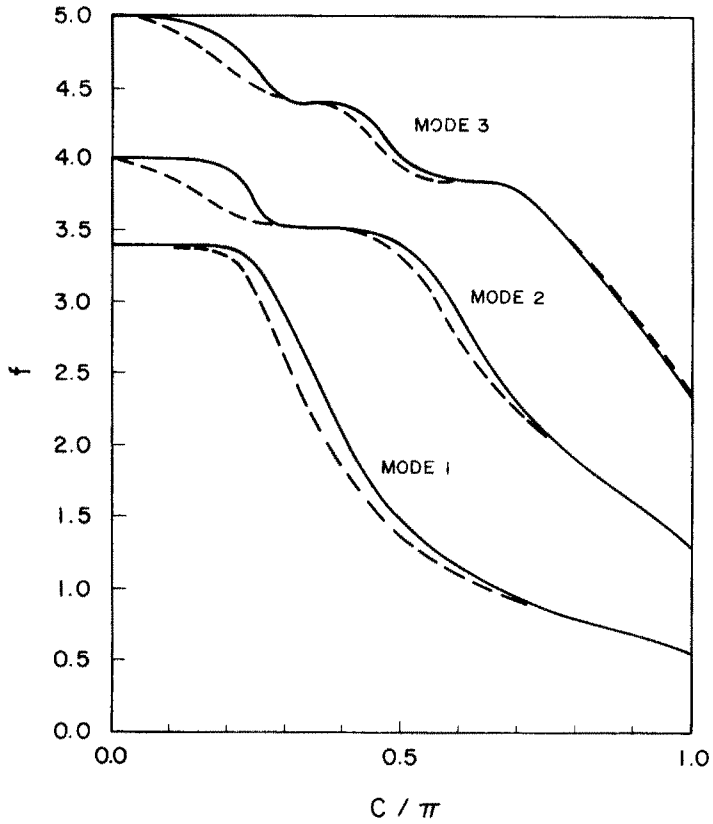

FIG. 3. Frequency factor vs. crack length for plate with crack from one edge. Vibration modes antisymmetric in y. $\gamma = 2{\cdot}0$.

of Ref. [3] does not account for the singularity of the solution, the agreement between the two methods with regard to the global quantities such as frequency is seen to be quite reasonable.

For the symmetric vibration modes of the plate with a crack from one edge, relative moment distributions were also calculated according to (33) and they are shown by the solid lines on Figs. 4–6. Superimposed by the dashed lines are the moment distributions taken from Ref. [3]. It is seen that good agreement exists away from the crack tip. Close to the crack tip, however, the moment distributions differ quite drastically. This indicates that even though global quantities such as frequency can be computed reasonably well by methods which do not account for the singularity, it is extremely difficult to accurately compute point-wise quantities such as the moment distribution in the vicinity of the point where the boundary conditions are discontinuous. Finally, the contours of constant deflection for the first three symmetric vibration modes are illustrated in Fig. 7.

The buckling factors for the plate with a crack from one edge are tabulated in Table 3. Figure 8 illustrates the buckling mode shapes for three different crack lengths. It is interesting

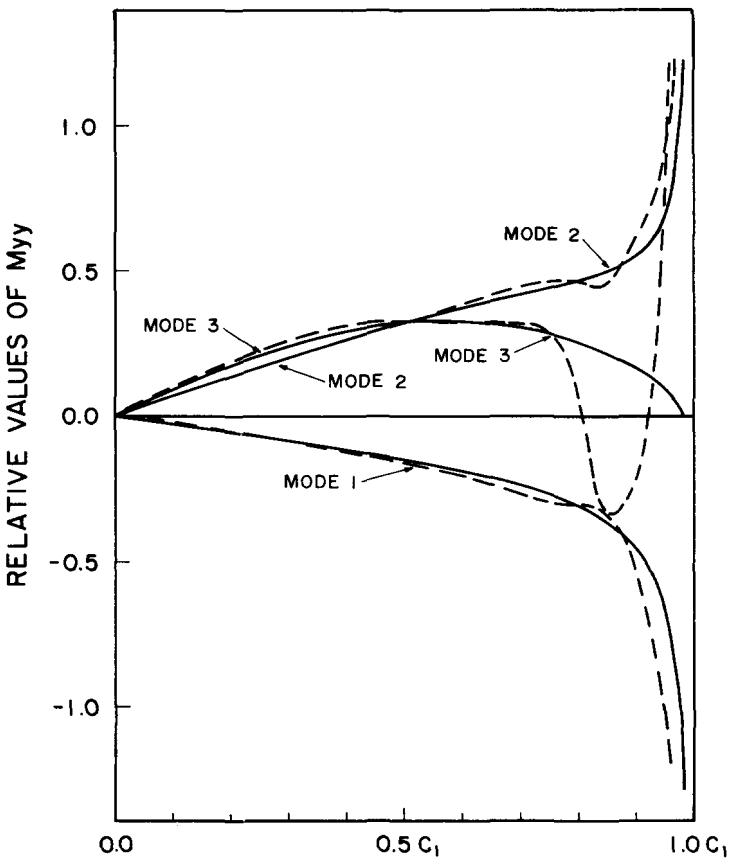

FIG. 4. Moment distribution along uncracked segment c_1 for plate with crack from one edge. Vibration modes symmetric in y. $c_1 = 0{\cdot}3\pi$, $\gamma = 2{\cdot}0$.

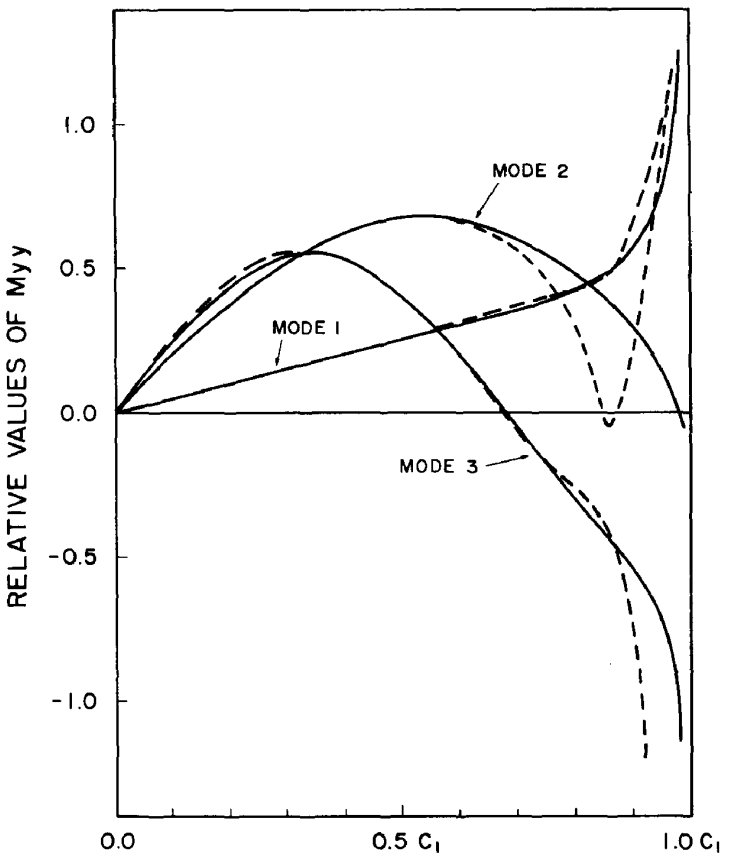

FIG. 5. Moment distribution along uncracked segment c_1 for plate with crack from one edge. Vibration modes symmetric in y. $c_1 = 0{\cdot}5\pi$, $\gamma = 2{\cdot}0$.

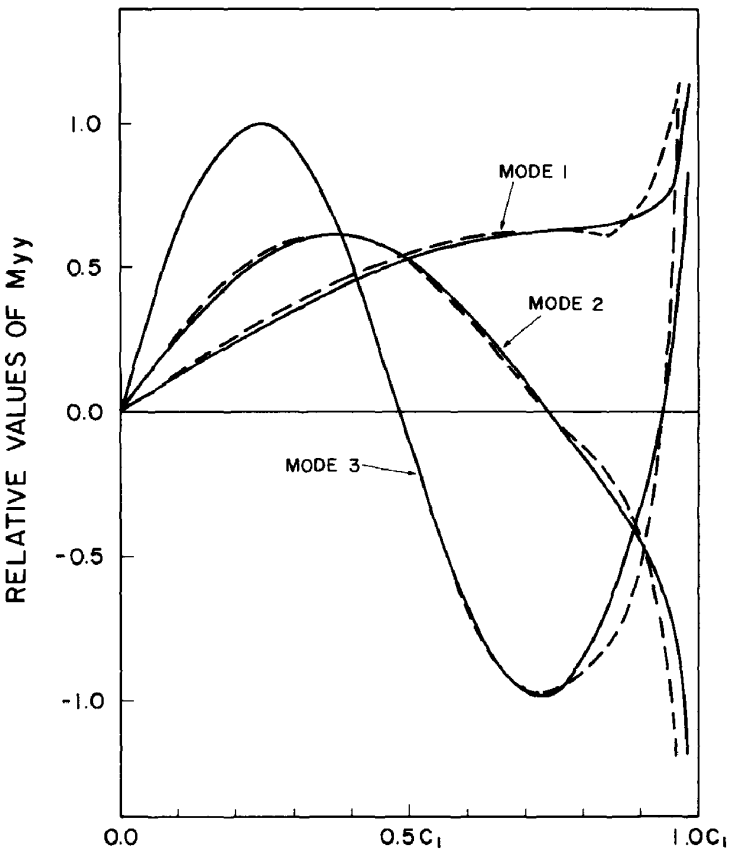

FIG. 6. Moment distribution along uncracked segment c_1 for plate with crack from one edge. Vibration modes symmetric in y. $c_1 = 0{\cdot}7\pi$, $\gamma = 2{\cdot}0$.

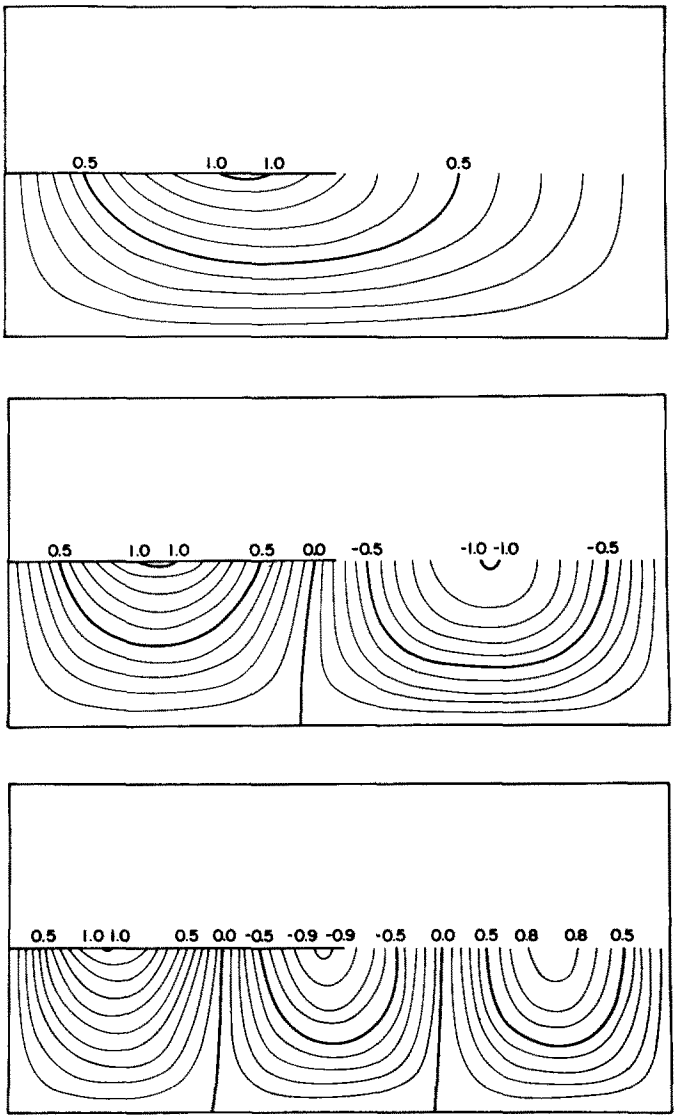

FIG. 7. Contours of constant deflection for symmetric vibration of plate with crack from one edge. $c = 0{\cdot}5\pi, \gamma = 2{\cdot}0$. Upper: mode 1; middle: mode 2; lower: mode 3.

to observe that when the crack length is small, the buckled shape has two semiwaves in the x-coordinates. As the crack length increases, the buckled shape goes into one semiwave.

Tables 4–7 summarize the numerical results for the vibration modes of the plate with an internal crack. The modes are numbered according to the number of semiwaves that occur in the x-coordinate when the plate is uncracked. The letters behind the numbers differentiate modes having different number of semiwaves in the y-coordinate. The buckling factors for the plate with an internal crack are tabulated in Table 8.

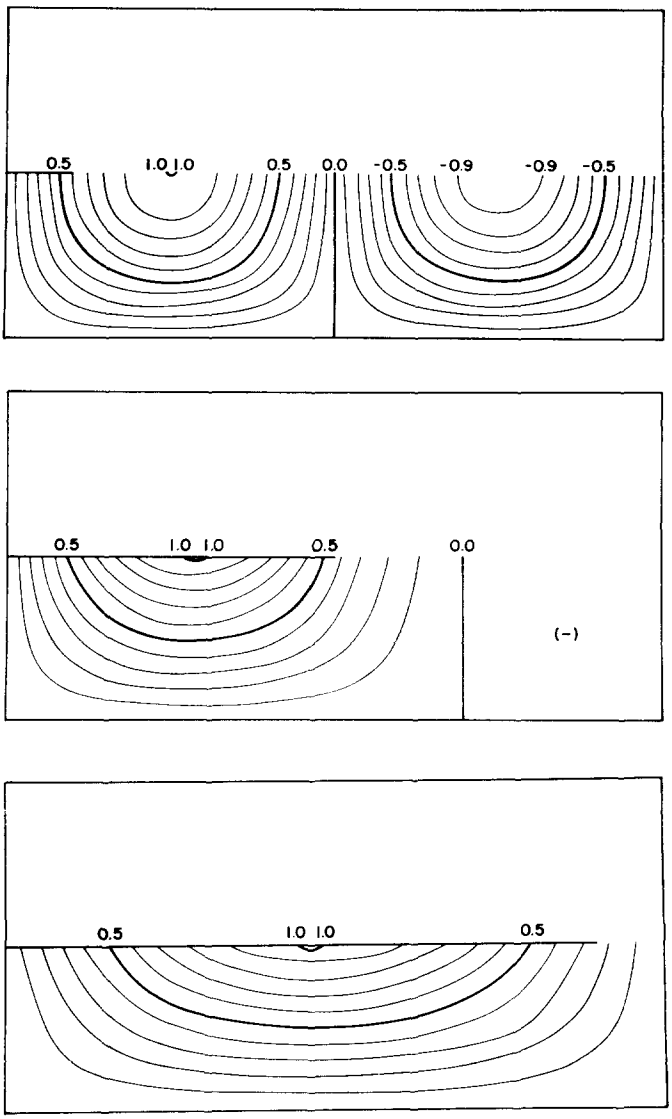

FIG. 8. Contours of constant deflection for buckling mode of plate with crack from one edge. Upper: $c = 0{\cdot}1\pi, \gamma = 2{\cdot}0$; middle: $c = 0{\cdot}5\pi, \gamma = 2{\cdot}0$; lower: $c = 0{\cdot}9\pi, \gamma = 2{\cdot}0$.

Acknowledgements—The first author is grateful to the National Science Foundation and Northwestern University for financial support during his tenure as a graduate student.

REFERENCES

[1] L. M. KEER and C. SVE, On the bending of cracked plates. *Int. J. Solids Struct.* **6**, 1545–1559 (1970).
[2] R. A. WESTMANN and W. H. YANG, Stress analysis of cracked rectangular beams. *J. appl. Mech.* **34**, 693–701 (1967).
[3] P. P. LYNN and N. KUMBASAR, Free Vibrations of Thin Rectangular Plates Having Narrow Cracks with Simply Supported Edges, in *Developments in Mechanics*, Vol. 4, Proc. Tenth Midwestern Mechanics Conference, Colorado State University, Fort Collins, Colorado, August 21–23, pp. 911–928 (1967).

[4] S. H. CRANDALL, *Engineering Analysis*. McGraw-Hill (1956).
[5] S. S-H. CHEN and G. PICKETT, Bending of plates of any shape and with any variation in boundary conditions. *J. appl. Mech.* **34**, 217–218 (1967).
[6] S. S-H. CHEN and G. PICKETT, Bending of Uniform Plates of Arbitrary Shapes and with Mixed Boundary Conditions, in *Developments in Mechanics*, Vol. 4, Proc. Tenth Midwestern Mechanics Conference, Colorado State University, Fort Collins, Colorado, August 21–23, pp. 411–427 (1967).
[7] A. W. LEISSA, W. E. CLAUSEN, L. E. HULBERT and A. T. HOPPER, A comparison of approximate methods for the solution of plate bending problems. *AIAA Jnl.* **7**, 920–928 (1967).
[8] J. N. GOODIER, The influence of circular and elliptical holes on the transverse flexure of elastic plates. *Phil. Mag.* **22**, 69–80 (1936).
[9] G. C. SIH, P. C. PARIS and F. ERDOGAN, Crack-tip, stress-intensity factors for plane extension and plate bending problems. *J. appl. Mech.* **29**, 306–312 (1962).
[10] Y. Y. YU, The Influence of a Small Hole or Rigid Inclusion on the Transverse Flexure of Thin Plates, *Proc. Second U.S. National Congress of Applied Mechanics*, pp. 381–387 (1954).
[11] M. L. WILLIAMS, The bending stress distribution at the base of a stationary crack. *J. appl. Mech.* **28**, 78–82 (1961).
[12] M. L. WILLIAMS, Surface Stress Singularities Resulting from Various Boundary Conditions in Angular Corners of Plates Under Bending, *U.S. National Congress of Applied Mechanics*, Illinois Institute of Technology, Chicago, Illinois, pp. 325–329 (1952).
[13] S. TIMOSHENKO and S. WOINOWSKY-KRIEGER, *Theory of Plates and Shells*, 2nd edition. McGraw-Hill (1959).
[14] I. S. GRADSHTEYN and I. M. RYZHIC, *Tables of Integrals, Series and Products*, 4th edition, p. 427. Academic Press (1965).
[15] C. SVE and L. M. KEER, Indentations of an elastic layer by moving punches. *Int. J. Solids Struct.* **5**, 795–816 (1969).
[16] G. C. SIH and J. F. LOEBER, Torsional vibration of an elastic solid containing a penny-shaped crack. *J. acoust. Soc. Am.* **44**, 1237–1245 (1968).
[17] S. D. CONTE, *Elementary Numerical Analysis*. McGraw-Hill (1965).

(*Received* 17 *December* 1970; *revised* 3 *June* 1971)

Абстракт—Работа рассматривает вопрос задач на собственные значения, касающихся прямоугольных пластинок с трещинами. Решаются задачи колебаний и устойчивости, для пластинки с трещиной, распространяющейся от края и для пластинки с концентрически расположеной вкутренней трещиной. Задачи формулируются в форме уравнений в парных рядях и сводятся к однородным интегральным уравнениям фредгольма второго рода. Для каждого случая выделяется сингулярность рещения и затем определяется анилитически. Сравниваются числённые результаты для собственных частот и распределение моментов, с работой других исследователей. Иллюстрируются формы колебаний и выпучивания для пластинки с трещиной.